

Article

Influence of the Water-Cooled Heat Exchanger on the Performance of a Pulse Tube Refrigerator

Wei Wang ^{1,2}, Jianying Hu ^{1,*}, Jingyuan Xu ^{1,2}, Limin Zhang ¹ and Ercang Luo ¹

¹ TKey Laboratory of Cryogenics, Technical Institute of Physics and Chemistry, Chinese Academy of Sciences, Beijing 100190, China; wangwei13@mails.ucas.ac.cn (W.W.); xujingyuan@mail.ipc.ac.cn (J.X.); liminzhang@mail.ipc.ac.cn (L.Z.); ecluo@mail.ipc.ac.cn (E.L.)

² The College of Materials Science and Opto-electronic Engineering, University of Chinese Academy of Sciences, Beijing 100049, China

* Corresponding: jyhu@mail.ipc.ac.cn; Tel.: +86-10-8254-3733

Academic Editor: Artur Jaworski

Received: 4 January 2017; Accepted: 23 February 2017; Published: 28 February 2017

Abstract: The water-cooled heat exchanger is one of the key components in a pulse tube refrigerator. Its heat exchange effectiveness directly influences the cooling performance of the refrigerator. However, effective heat exchange does not always result in a good performance, because excessively reinforced heat exchange can lead to additional flow loss. In this paper, seven different water-cooled heat exchangers were designed to explore the best configuration for a large-capacity pulse tube refrigerator. Results indicated that the heat exchanger invented by Hu always offered a better performance than that of finned and traditional shell-tube types. For a refrigerator with a working frequency of 50 Hz, the best hydraulic diameter is less than 1 mm.

Keywords: heat exchanger; pulse tube refrigerator; shell-tube types

1. Introduction

Owing to their high reliability, high efficiency, and compact size, pulse tube refrigerators have attracted much attention in the past decades [1]. Many of them have been developed to cool devices such as infrared detectors, HTS filters, and germanium detectors. Their cooling power is often less than ten watts. Recent advances in high-temperature superconductivity (HTS) devices, small gas liquefaction, and cryogenic storage tanks, have spurred the demand for high-capacity refrigerators. The cooling power required by such applications varies from hundreds to thousands of watts, and the corresponding cooling temperature varies from 80 to 120 K [2–4]. The pulse tube refrigerator was considered to be one of the best candidates, so the development and use of high-capacity pulse tube refrigerators boomed. At present, the cooling power of these refrigerators can exceed 1 kW at a temperature of 80 K, and a relative Carnot efficiency of 22% has been achieved [5–9]. Although this efficiency is quite high, some studies have indicated that the room temperature heat exchanger could be further improved [10–12].

The water-cooled heat exchanger (WCHX) is one of the core components in a pulse-tube cooler [13,14]. The function of the heat exchanger is to transfer time-averaged heat from the gas to the water, which acts as an external heat sink. It must provide good thermal contact between the two flowing streams, while causing a minimal pressure drop in either stream. There are three typical configurations for water-cooled heat exchangers employed in pulse tube refrigerators. The first is the finned-tube type introduced in References [15,16]. In this type, fins of different lengths are arranged in a round case at regular intervals. Thermal contact between the fins and tubes acting as channels for the water is ensured by soldering. Although this is a very appropriate high-capacity design in theory, it is technically difficult. The water-cooled heat exchanger presented in References [17–19], shown in

Figure 1b, can also be considered a fin-tube type. The fins are machined by wire electrical discharge machining (WEDM), and the water only flows around the circumference of the case. Meanwhile, the temperature difference on the fins caused by heat conductance will increase with the size of the exchanger [8,20]. It is much easier to machine, but more expensive. The third configuration is the shell-tube type, shown in Figure 1c. As is known, the heat transfer coefficient at the water side is much higher than that at the gas side [21], so the heat exchange at the gas side should be strengthened. With the present machining process capability, it is impossible to produce such fins in a pipe with a small hydraulic diameter. If the hydraulic diameter is less than 1 mm, the flow area of the gas is often less than 15% of the cross-sectional area of the heat exchanger. To overcome this drawback of the shell-tube heat exchanger, Hu introduced another configuration, as shown in Figure 1d [22]. Small tubes acting as fins are welded inside the larger tubes, to strengthen the heat transfer at the gas side. Because the fins are not long, a uniform temperature distribution on the heat exchanger can be ensured. The hydraulic diameter and flow area can be easily adjusted by changing the parameters of the small tubes. The effectiveness of this configuration was confirmed in Reference [19].

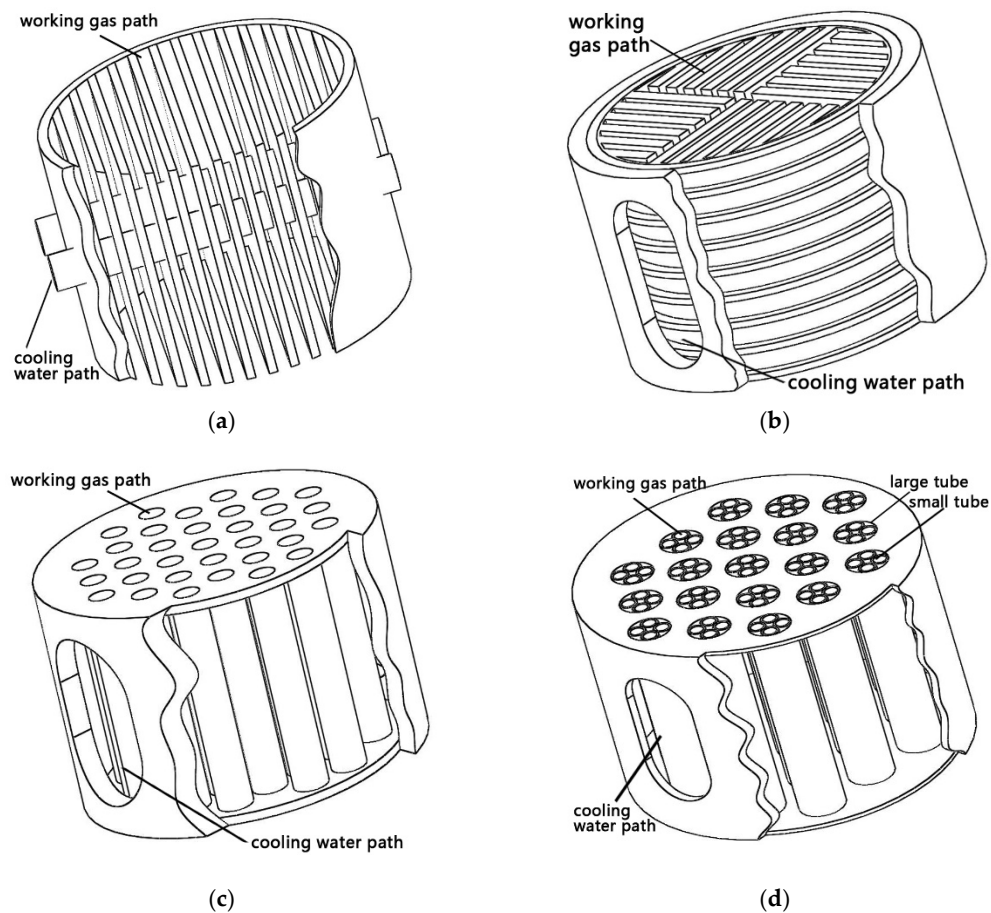


Figure 1. Four configurations of WHCXs. (a) Finned-tube type; (b) WEDM machined type which can be considered as a finned-tube type; (c) shell-tube type; (d) new type introduced by Hu.

Generally, a smaller hydraulic diameter and high flow velocity can improve heat transfer, but also result in greater flow loss. A good design achieves a reasonable compromise between these variables, in order to obtain the best performance of the refrigerator. The pressure drop can be calculated based on thermoacoustic theory. Meanwhile, the heat transfer is hard to evaluate because the empirical correlation for steady flow cannot be directly applied. A well accepted heat transfer correlation for oscillating flow is still absent, although much investigation has been carried out in this

area [13,18,23,24]. Thus, in this work, we used experiments to determine the influence of factors such as the hydraulic diameter, length, contact thermal resistance, and porosity, on the cooling performance of a pulse tube refrigerator.

2. Experimental Apparatus and WCHXs

2.1. Experimental Apparatus

The experimental apparatus is schematically shown in Figure 2. It mainly consisted of a linear compressor and an in-line pulse-tube cooler. The main geometric parameters of the cooler and its operating conditions are listed in Table 1. The water-cooled heat exchanger was replaceable, so that different heat exchangers could be tested. The heat exchangers were cooled by circulating water with a temperature of 293 K. Because the hydraulic diameter of the heat exchanger was quite small, it was difficult to place thermometers inside it, in order to measure the gas or the wall temperatures. Subsequently, only a calibrated K-type sheathed thermocouple (T_0) was installed close to the inlet of the heat exchanger, to measure the gas temperature.

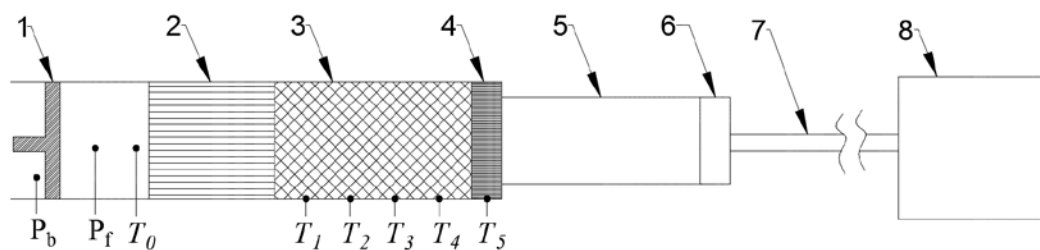


Figure 2. Schematic of the experimental apparatus. 1 Liner compressor; 2 WCHX; 3 Regenerator; 4 Clod head; 5 Pulse-tube; 6 Flow straightener; 7 Inertance tube; 8 Gas reservoir.

The regenerator housing was filled with a 300-mesh stainless-steel screen with a porosity of 0.7. Four calibrated PT-100 resistance thermometers (T_1 – T_4) with an accuracy of ± 0.1 K were placed on the outer wall of the regenerator, distributed with equal spacing. If the wall temperature equals the screen temperature in the same cross-section, then the temperature in the regenerator can be obtained from the four thermometers. The temperature of the cold head was measured with another PT-100 (T_5). Three constantan wires heated by a direct voltage source were mounted on the cold head, to simulate cooled loads. The voltage was adjusted to keep the temperature of the cold head at 80 K. The heat power was read from the direct voltage source, which had an accuracy of $\pm 0.3\%$. The regenerator, cold head, and pulse tube, were enclosed in a vacuum chamber. The flow straightener was made of 5-mm long 40-mesh copper screens. The inertance tube was cooled with a water jacket. The linear compressor was used to provide acoustic power for the pulse-tube cooler. The efficiency of the compressor was not important in this study, so the match between the compressor and the refrigerator was not optimized. The output acoustic power of the compressor was calculated from the pressures (P_f and P_b , respectively) in its front and back spaces. P_f and P_b were measured using high-precision dynamic pressure sensors, supplied by PCB Piezotronics shown in Figure 2. The input acoustic power, W_a , was calculated as:

$$W_a = \frac{1}{2} \left| P_f \right| \left| \frac{i\omega V_b}{\gamma P_0} P_b \right| \cos \theta_{PU} \quad (1)$$

where θ_{PU} is the phase difference between the pressure wave and the volume flow rate, ω is the angular frequency, V_b is the back space volume of the compressor, P_0 is the mean pressure, and γ is the specific heat ratio [25]. The accuracy of the pressure sensor measuring P_0 was 0.2%. The non-linearity of the pressure sensors measuring P_f and P_b was 1%.

Table 1. Operating conditions and component size.

Item	Item	Value
Operating condition	Working gas	helium
	Operating pressure	3 MPa
	Frequency	55 Hz
	Cooling temperature	80 K
Component size	Regenerator	75 × 70 (300 mesh)
	Pulse tube	37 × 150
	Cold head	75 × 30
	Inertance tubes	10 × 2300

All listed dimensions are inner diameter × length (all in mm).

2.2. Water-Cooled Heat Exchangers

Figure 3 shows cross-sectional photographs of the WHCXs used in the experiment. The details of each WHCX are presented in Table 2. WCHX 1 was machined by WEDM. It can be considered a finned-tube type. WCHX 2 had a traditional shell-tube structure, while WCHXs 3–6 were the new shell-tube types introduced by Hu. In WCHX 3, the small tubes acting as fins in the large tubes were larger than those in WCHX 4, so were deformed during processing. They were more triangular than circular. WCHX 5 and 6 had the same gas channels as WCHX 4, so their photographs are not shown in Figure 3. WCHX 4 and WCHX 5 had the same parameters. The only difference was that in WCHX 4, the small tubes were welded to the large tubes (before processing, the welder was electroplated to the outer surface of the small tubes). In WCHX, the small and large tubes were just touching, without welding (Please refer to Reference [14] for the processing details). To remove the influence of different gas velocities, the porosity (area of gas channel to cross-sectional area) was maintained at about 25%. With this porosity, the gas velocity varied from 10 to 29 m/s, when the input acoustic power was changed from 1280 to 5000 W. To investigate the influence of porosity, some channels were blocked with thin round plates in WCHX 7.

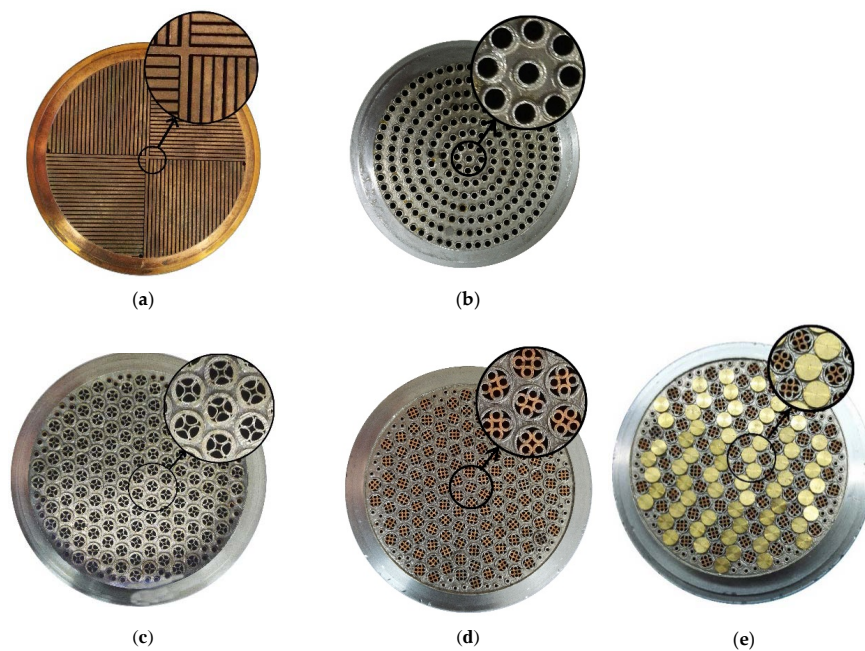


Figure 3. Photographs of (a) WCHX 1; (b) WCHX 2; (c) WCHX 3; (d) WCHX 4; and (e) WCHX 7. WCHXs 5 and 6 had the same gas channels as WCHX 4.

Table 2. Parameters of the WHCXs.

WHCX	Porosity	Gas-solid Heat Transfer Area	Hydraulic Diameter	Length	Remarks
1	26.2%	0.38 m ²	0.8 mm	64 mm	-
2	23.8%	0.11 m ²	2.44 mm	64 mm	-
3	25.1%	0.261 m ²	1.35 mm	64 mm	-
4	24.5%	0.386 m ²	0.76 mm	64 mm	-
5	24.5%	0.386 m ²	0.76 mm	64 mm	No welding between small and big tubes
6	24.5%	0.193 m ²	0.76 mm	32 mm	-
7	12.3%	0.193 m ²	0.76 mm	64 mm	-

3. Experimental Results

3.1. Influence of Different Configurations

To study the effect of the structure of the water cooler on the heat transfer performance, the performance of WCHX 1, WCHX 2, and WCHX 4, were compared. Figure 4 presents the dependence of the overall relative Carnot efficiency η on the input acoustic power.

$$\eta = \frac{Q(T_h - T_c)}{W_a T_c} \tag{2}$$

where Q is the cooling power, T_c is the cold head temperature, and T_h is the cooling water temperature. A better cooling performance was achieved when WCHX 4 was used. When the input acoustic power was about 1500 W, the system performance was similar for WCHX 1 and WCHX 2; with a larger input acoustic power, the performance with WCHX 2 was better than that with WCHX 1; however, there was still a gap with that observed with WCHX 4. This was apparent in high-power conditions, where WCHX 4 had a great advantage compared with the other two WCHXs. Taking an input acoustic power of 4000 W as an example, the WCHX 4 system achieved a relative Carnot efficiency of 20.6% and cooling power of 319 W, whereas the system with WCHX 1 only achieved an efficiency of 18% and cooling power of 270 W, and the system with WCHX 2 only achieved an efficiency of 18.7% and cooling power of 281 W.

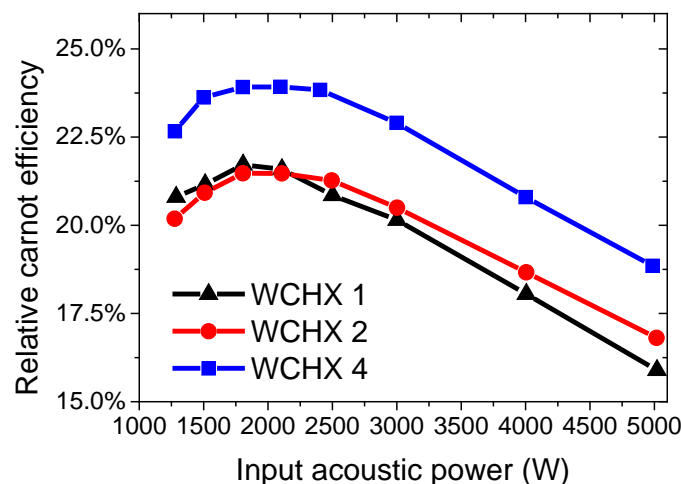


Figure 4. Dependence of relative Carnot efficiency on input acoustic power for WCHXs 1, 2, and 4.

Owing to the aforementioned technical difficulty, the gas temperature was measured at the inlet of the WCHXs, as shown in Figure 5. At 1270 W input acoustic power, there was no large difference in gas temperature among the three WCHX designs: 35 °C with WCHX 1, 24 °C with WCHX 2,

and 23 °C with WCHX 4. The gas temperature increased with the input acoustic power, especially in the system with the plated-fin WCHX. When the input acoustic power was 5000 W, the gas temperature was as high as 76 °C with WCHX 1, but only 33 °C with WCHX 4. This implies that WCHX 4 was better cooled.

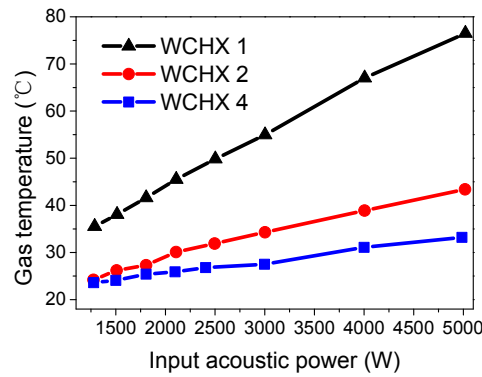


Figure 5. Gas temperatures at the inlets of WCHXs 1, 2, and 4.

What puzzled us is that the gas temperature obtained with WCHX 2 was very close to that with WCHX 4 (Figure 5), but its efficiency was closer to that of WCHX 1 (Figure 4). The temperature distribution along the regenerator shown in Figure 6 may provide some explanations. The x -axis begins at the warm end of the regenerator and ends at its cold end. The data points are the temperatures measured by thermometers T_1 to T_4 , and the straight lines are their fitted results. At an input acoustic power of 1270 W, the temperature at the warm end for WCHXs 1 and 2 were very close, and were 10 K higher than that for WCHX 4. This means that with WCHX 4, the temperature difference between the two ends of the regenerator was less, and thus, more cooling power was obtained. At an input acoustic power of 5000 W, the temperature at the warm end observed with WCHX 1 was about 10 K higher than that with WCHX 2, and about 24 K higher than that with WCHX 4. As a result, more effort was required to pump heat from the cold head to the ambient end of the regenerator. Figures 4–6 indicated that the more effective parameter to evaluate the performance of the WCHXs in a pulse tube refrigerator, is the hot-end temperature of the regenerator, instead of the inlet gas temperature of the WCHXs.

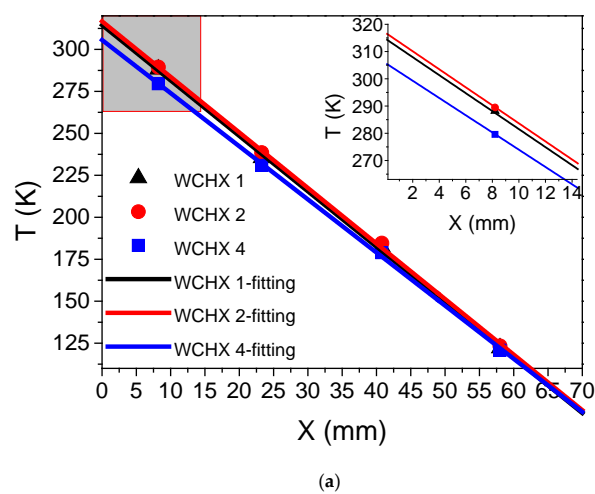


Figure 6. Cont.

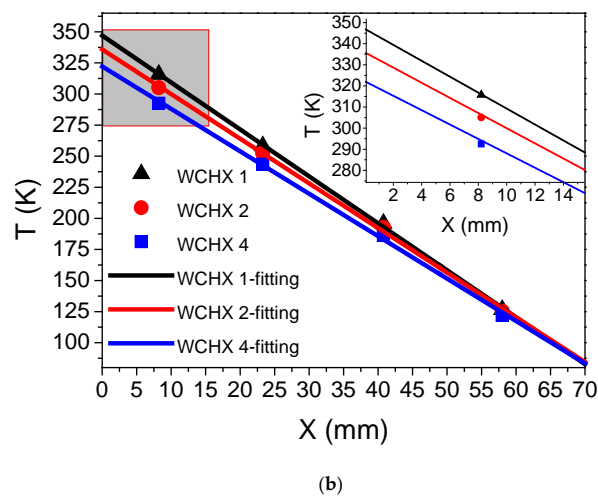


Figure 6. Temperature distribution in the regenerator at input acoustic power of (a) 1270 W and (b) 5000 W for WCHXs 1, 2, and 4.

3.2. Influence of Length

Generally, a longer WCHX means a greater heat transfer area, which is helpful for the overall heat transfer, but also results in a greater flow loss. So, an ideal WCHX is a compromise between heat transfer and flow loss. Figure 7 presents the relative Carnot efficiency of a refrigerator with two different length WCHXs. The length of WCHX 6 was half the length of WCHX 4. The system performance of the two WCHX designs was almost the same, because the warm-end temperatures of the regenerator were almost the same, as shown in Figure 8. Thus, the half length WCHX met the heat transfer requirements of the system. The gas temperature at the inlet of the WCHXs was also compared, as shown in Figure 9. The figure shows that the inlet gas temperature of WCHX 4 was smaller than the shorter WCHX 6. This was conducive for reducing the outlet gas temperature of the compressor, which has a positive impact on the stability of the system. From the aspects of improved performance and economy, there is no need to make the WCHX too long.

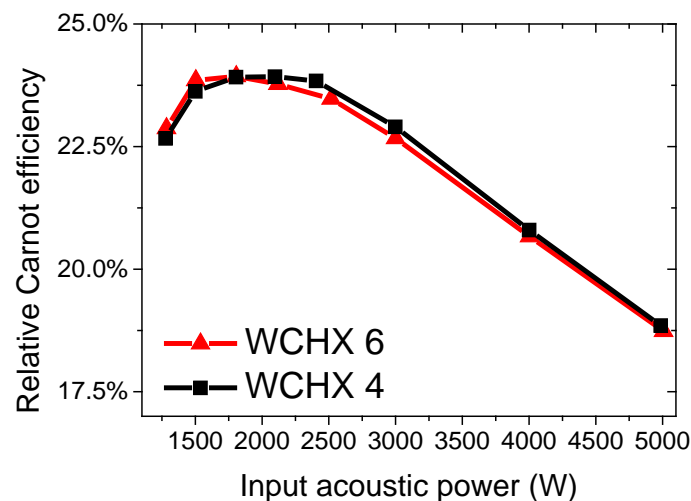


Figure 7. Dependence of relative Carnot efficiency on the input acoustic power for WCHXs 4 and 6.

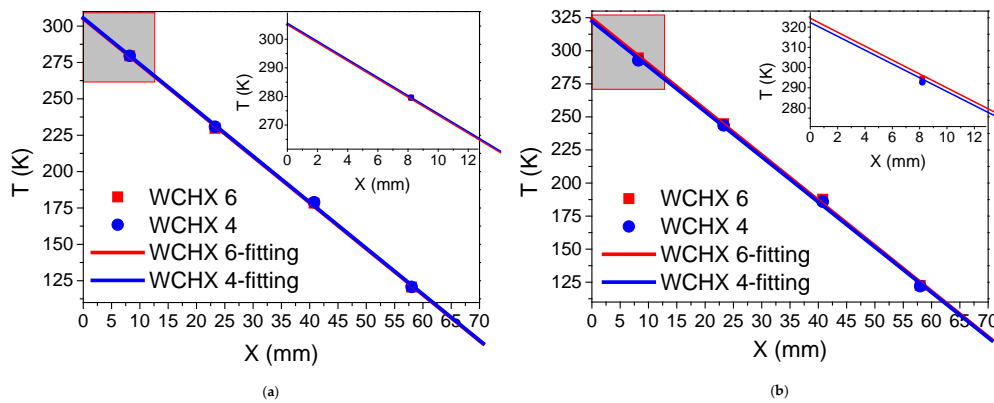


Figure 8. Temperature distribution in the regenerator at an input acoustic power of (a) 1270 W and (b) 5000 W, for WCHXs 4 and 6.

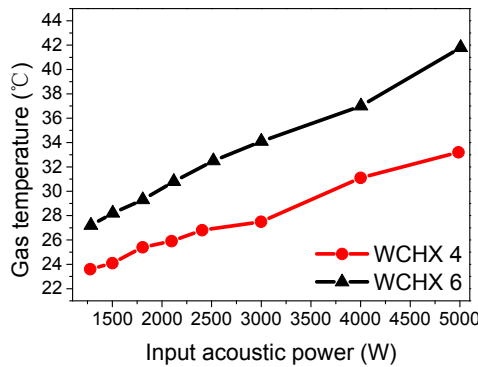


Figure 9. Gas temperature at the inlets of the WCHXs 4 and 6.

3.3. Influence of Different Contact Thermal Resistance WCHXs

In WCHX 4, the small tubes acted as fins and transferred heat to the wall of the large tubes, so the heat transfer between the small and large tubes had a significant impact. The small tubes should be welded to the larger tubes, to ensure the best thermal contact, but welding makes the machining process quite complex. If good thermal contact can be achieved by extrusion, the welding process can be omitted. Figure 10 presents the relative Carnot efficiency of the refrigerator with WCHXs 4 and 5. In WCHX 5, the small tubes were not welded to the large tubes. The performance of the two WCHXs was almost the same. This indicates that good thermal contact between the large and small tubes can be achieved by extrusion.

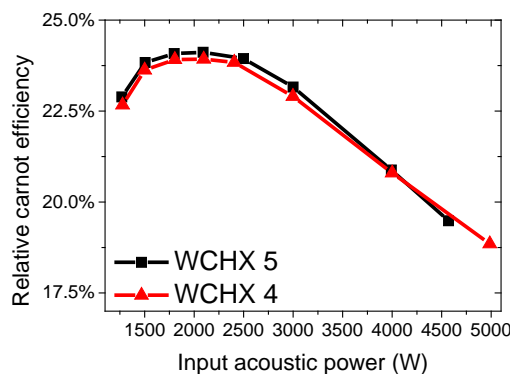


Figure 10. Dependence of relative Carnot efficiency on input acoustic power for WCHXs 4 and 5.

3.4. Influence of Different Hydraulic Diameter

From the definition of the heat transfer coefficient, we know that a smaller hydraulic diameter means a greater heat transfer coefficient, which is conducive to heat transfer. However, the flow resistance between the gas and the wall will be increased if the hydraulic diameter is too small, which will increase the loss in acoustic power. Therefore, the choice of an appropriate hydraulic diameter of the WCHX is very important. Figure 11 presents the relative Carnot efficiency of the refrigerator, with different hydraulic diameters (WCHXs 3 and 4). At the same acoustic power, a better cooling performance was achieved with WCHX 4, which had a smaller hydraulic diameter than WCHX 3. It should be noted that the actual heat transfer area of WCHX 3 was less than that of 4, and it was difficult to distinguish which was the more important factor for causing this different performance. When compared with WCHX 3, the heat transfer in WCHX 4 was increased by about 50%, and the hydraulic diameter was decreased from 1.35 mm to 0.76 mm, but the efficiency in Figure 11 only increased a little. Therefore, we did not think that it was necessary to further decrease the hydraulic diameter.

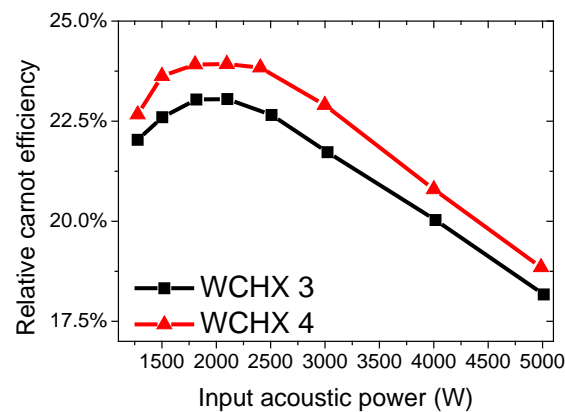


Figure 11. Dependence of relative Carnot efficiency on input acoustic power for WCHXs 3 and 4.

3.5. Influence of Different Porosity

A higher porosity of WCHXs is helpful for decreasing the flow resistance, but will lower the flow velocity and weaken the heat transfer. There were 142 large tubes and 568 small tubes in WCHX 4. There is no doubt that this is a huge number. If the WCHX can meet the heat transfer requirements of the system with a reduced number of tubes, it will save material and produce lower costs during processing. Therefore, we studied the effect of such a reduction on WCHX 4. Half of the gas flow channels were plugged, so that the porosity of the WCHX became 12.3% (WCHX 7). Figure 12 presents the relative Carnot efficiency of the refrigerator with WCHXs 4 and 7. Figure 12 shows that, at the same acoustic power, a better cooling performance was achieved when WCHX 4 was used. Compared with WCHX 7, the porosity and heat transfer area in WCHX 4 was doubled. It can be seen that the efficiency improvement was not significant. The efficiency improvement can be partly explained by the increase of the heat transfer area. Therefore, we loosely argue that the porosity effect is not significant in this experiment. However, it may seriously affect the flow loss and flow inhomogeneity in the regenerator, if the porosity is too small.

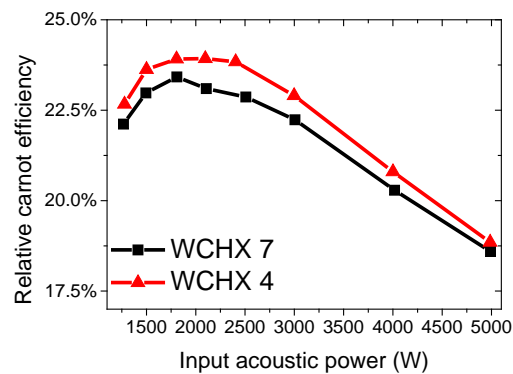


Figure 12. Dependence of relative Carnot efficiency on input acoustic power for WCHXs 4 and 7.

4. Conclusions

Several WCHXs were tested for their use in a high-capacity pulse-tube cooler. The performance of the pulse tube refrigerator with differently structured WCHXs was compared and analyzed. It was found that the warm-end temperature of the regenerator, instead of the gas temperature at the inlet of the WCHX, influenced the cooling performance of the refrigerator. Owing to its more uniform fin temperature distribution, smaller hydrodynamic diameter, and greater heat transfer area, the WCHX design invented by Hu always outperformed the plated-fin and traditional shell-tube type WCHXs. With this WCHX in a pulse tube refrigerator working at a frequency of about 55 Hz, a hydraulic diameter of 0.76 mm, length of 32 mm, and porosity of 24.5%, were appropriate. It was also found that the welding process could be omitted because good thermal contact was achieved by extrusion. This will be helpful for lowering the cost of this configuration. The configuration is suitable for consideration for further use in other regenerative prime movers and coolers.

Acknowledgments: This work was supported by the National Natural Science Foundation of China (Grant No. 51576204) and National Key Research and Development Program of China (Contract No. 2016YFB0901403).

Author Contributions: Jianying Hu, Limin Zhang and Ercang Luo conceived and designed the experiments; Wei Wang and Jingyuan Xu performed the experiments; Wei Wang analyzed the data; Wei Wang and Jianying Hu wrote the paper.

Conflicts of Interest: The authors declare no conflict of interest.

References

- Gifford, W.E.; Longsworth, R.C. Pulse-tube refrigeration. *J. Eng. Ind.* **1964**, *86*, 264–268. [[CrossRef](#)]
- Zia, J.H. A commercial pulse tube cryocooler with 200 W refrigeration at 80 K. In *Cryocoolers 13*; Ross, R.G., Ed.; Springer: Boston, MA, USA, 2005; pp. 165–171.
- Zia, J.H. A pulse tube cryocooler with 300 W refrigeration at 80 K and an operating efficiency of 19% carnot. *Cryocoolers* **2007**, *14*, 141–147.
- Hu, J.Y.; Zhang, L.M.; Zhu, J.; Chen, S.; Luo, E.C.; Dai, W.; Li, H.B. A high-efficiency coaxial pulse tube cryocooler with 500 W cooling capacity at 80 K. *Cryogenics* **2014**, *62*, 7–10. [[CrossRef](#)]
- Potratz, S.A.; Nellis, G.F.; Maddocks, J.R.; Kashani, A.; Helvensteijn, B.P.M.; Rhoads, G.L.; Flake, B. Development of a large-capacity, stirling-type, pulse-tube refrigerator. *AIP Conf. Proc.* **2006**, *823*, 3–10.
- Potratz, S.A.; Abbott, T.D.; Johnson, M.C.; Albaugh, K.B. Stirling-type pulse tube cryocooler with 1 kW of refrigeration at 77 K. *AIP Conf. Proc.* **2008**, *985*, 42–48.
- Hu, J.Y.; Luo, E.; Wu, Z.; Yu, G.; Dai, W. Design of a large-capacity multi-piston pulse tube cryocooler. *AIP Conf. Proc.* **2012**, *1434*, 540–546.
- Hu, J.Y.; Chen, S.; Zhu, J.; Zhang, L.M.; Luo, E.C.; Dai, W.; Li, H.B. An efficient pulse tube cryocooler for boil-off gas reliquefaction in liquid natural gas tanks. *Appl. Energy* **2015**, *164*, 1012–1018. [[CrossRef](#)]

9. Caughley, A.; Emery, N.; Nation, M.; Allpress, N.; Kimber, A.; Branje, P.; Reynolds, H.; Boyle, C.; Meier, J.; Tanchon, J. Commercial pulse tube cryocoolers producing 330 W and 1000 W at 77 K for liquefaction. *IEEE Trans. Appl. Supercond.* **2016**, *26*, 1–4. [[CrossRef](#)]
10. Bretagne, E.; François, M.X.; Ishikawa, H. Investigations of acoustics and heat transfer characteristics of thermoacoustic driven pulse tube refrigerators. *AIP Conf. Proc.* **2004**, *710*, 1687–1695.
11. Ki, T.; Jeong, S. Optimal design of the pulse tube refrigerator with slit-type heat exchangers. *Cryogenics* **2010**, *50*, 608–614. [[CrossRef](#)]
12. Yang, K.X.; Wu, Y.N.; Zhang, A.K.; Xiong, C. Fabrication of Taper Gap Warm End Heat Exchanger in Coaxial Pulse Tube Cryocooler. *Adv. Mater. Res.* **2012**, *591–593*, 365–368. [[CrossRef](#)]
13. Chen, Y.Y.; Luo, E.C.; Dai, W. Heat transfer characteristics of oscillating flow regenerator filled with circular tubes or parallel plates. *Cryogenics* **2007**, *47*, 40–48. [[CrossRef](#)]
14. Gholamrezaei, M.; Ghorbanian, K. Thermal analysis of shell-and-tube thermoacoustic heat exchangers. *Entropy* **2016**, *18*, 301. [[CrossRef](#)]
15. Kamsanam, W.; Mao, X.; Jaworski, A.J. Thermal performance of finned-tube thermoacoustic heat exchangers in oscillatory flow conditions. *Int. J. Therm. Sci.* **2016**, *101*, 169–180. [[CrossRef](#)]
16. Jaworski, A.J.; Piccolo, A. Heat transfer processes in parallel-plate heat exchangers of thermoacoustic devices—numerical and experimental approaches. *Appl. Therm. Eng.* **2012**, *42*, 145–153. [[CrossRef](#)]
17. Tang, K.; Yu, J.; Jin, T.; Gan, Z.H. Influence of compression-expansion effect on oscillating-flow heat transfer in a finned heat exchanger. *J. Zhejiang Univ. Sci. A* **2013**, *14*, 427–434. [[CrossRef](#)]
18. Tang, K.; Yu, J.; Jin, T.; Wang, Y.P.; Tang, W.T.; Gan, Z.H. Heat transfer of laminar oscillating flow in finned heat exchanger of pulse tube refrigerator. *Int. J. Heat Mass Transfer* **2014**, *70*, 811–818. [[CrossRef](#)]
19. Xu, J.Y.; Hu, J.Y.; Zhang, L.M.; Luo, E. A novel shell-tube water-cooled heat exchanger for high-capacity pulse-tube coolers. *Appl. Therm. Eng.* **2016**, *106*, 399–404. [[CrossRef](#)]
20. Luo, L.A.; D’Ortona, U.; Tondeur, D. Compact heat exchangers. In *Microreaction Technology: Industrial Prospects: Imret 3: Proceedings of the Third International Conference on Microreaction Technology*; Ehrfeld, W., Ed.; Springer: Berlin/Heidelberg, Germany, 2000; pp. 556–565.
21. Kuppan, T. *Heat Exchanger Design Handbook*, 2nd ed.; CRC Press: Boca Raton, FL, USA, 2013; p. 21.
22. Hu, J.Y.; Long, X.D.; Li, H.B. Heat exchanger, oscillation flow system and heat exchanger processing methods, CN104964585A [P/OL]. 2015.
23. Bouvier, P.; Stouffs, P.; Bardon, J.-P. Experimental study of heat transfer in oscillating flow. *Int. J. Heat Mass Transfer* **2005**, *48*, 2473–2482. [[CrossRef](#)]
24. Chen, Y.; Luo, E.; Dai, W. Heat transfer characteristics of oscillating flow regenerators in cryogenic temperature range below 20 K. *Cryogenics* **2009**, *49*, 313–319. [[CrossRef](#)]
25. Hu, J.Y.; Wang, W.; Luo, E.C.; Chen, Y.Y. Acoustic field modulation in regenerators. *Cryogenics* **2016**, *80*, 1–7. [[CrossRef](#)]

